Magnesium Technology 2014
Edited by: Martyn Alderman, Michele V. Manuel, Norbert Hort, and Neale R. Neelameggham
TMS (The Minerals, Metals & Materials Society), 2014

HARDENING AND SOFTENING PROCESSES IN AN AJ51 MAGNESIUM ALLOY REINFORCED WITH SHORT SAFFIL FIBRES

Zuzanka Trojanová, Gergely Farkas, Kristián Máthis and Pavel Lukáč
Department of Physics of Materials, Faculty of Mathematics and Physics, Charles University in Prague,
Ke Karlovu 5, CZ-121 126 Praha 2, Czech Republic

Magnesium alloy, Metal matrix composite, Strengthening, Twinning, Residual stresses

Abstract

AJ51 alloy (5Al-0.6Sr balance Mg in wt.%) reinforced with short δ-Al_2O_3 fibres (Saffil®) has been deformed in compression at temperatures between 23 and 300 °C. The yield stress and the maximum stress decrease with increasing testing temperature. The influence of reinforcement on both characteristic stresses falls down with increasing temperature. Various strengthening terms were taken into account. Individual strengthening terms were calculated and compared with experimental results. Acoustic emission signal recorded during plastic deformation of the matrix alloy and composite was used to elucidate details of the plastic deformation in the matrix alloy and composite. Residual thermal stresses, generated due to a great difference between the thermal expansion coefficients of the alloy and ceramic reinforcement, in the composite matrix at different strain levels were estimated using neutron diffraction method.

Introduction

Magnesium alloys reinforced with short ceramic fibres combine good properties of both types of materials: a high stiffness of ceramic fibres and plasticity of metallic matrix [1]. Such materials have unique and desirable mechanical and physical properties [2]. Metal matrix composites (MMC) have higher stiffness [3, 4], higher strength [5, 6], better fatigue properties [7] and lower thermal expansion [8] than their metallic counterparts. On the other hand, plasticity of MMCs is lower, especially at lower temperatures. In spite of many attempts to reveal deformation mechanisms in composites and their link to microstructure of such materials, there is no comprehensive explanation of the role of the reinforcing phase in the plastic deformation of magnesium alloy based composites. New Mg-Al-Sr alloys are being developed with the aim to find cast alloys with good creep resistance and good strength alloys and replace expensive rare earth alloying elements with some cheaper one [9]. Further possibility how to improve mechanical properties of the Mg-Al-Sr alloys is to add the reinforcing phase and prepare a composite. Such materials have great potential in automotive, high performance defence and aerospace applications.
The main objective of this study is to investigate mechanical properties of an AJ51 magnesium alloy reinforced with short Saffil fibres with the aim to reveal the main features of the deformation mechanisms. Mechanical tests, acoustic emission (AE) and neutron diffraction (ND) were used.

Experimental

AJ51 alloy (the nominal chemical composition: Mg−5Al–0.6Sr in wt.%) was reinforced with δ-Al_2O_3 short fibres (Saffil). The preform consisting of Al_2O_3 short fibres showing a 2D planar isotropic fibre distribution and a binder system (containing Al_2O_3 and starch) were preheated to 1000 °C and then inserted into a preheated die (300-360 °C). Preforms were preheated and then infiltrated by the liquid alloy using two-stage application of the pressure. The mean fibre length and fibre diameter (measured after squeeze casting) were ~78 μm and ~3 μm, respectively. Volume fraction of fibres was estimated to be (17.9 ± 0.3) vol% Al_2O_3. Cylindrical samples were cut so that the stress axis was parallel to the fibres plane. Compression tests were carried out in an INSTRON universal testing machine with the displacement control at a nominal strain rate of 8.3×10^{-5} s^{-1} in a wide temperature range from room temperature (RT) to 300 °C. Fig. 1 shows microstructure of the composite studied taken from the section perpendicular to the fibres plane. The grain size exhibited in the non-deformed state for composite d_1 = (44±13) μm and d_2 = (110±30) μm for the alloy prepared with the same technology of the squeeze casting.

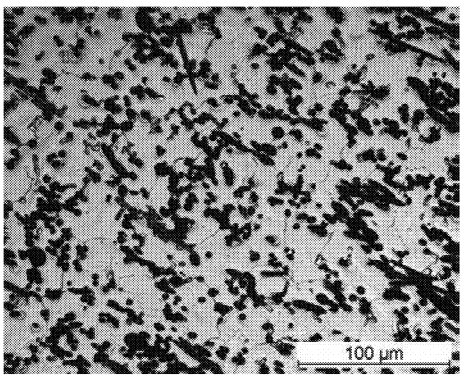

Fig. 1: Microstructure of the as cast sample (section perpendicular to the fibres plane).

The computer controlled DAKEL-XEDO-3 AE system was used to monitor AE on the basis of two-threshold-level detection, which yields a comprehensive set of AE parameters involving count rates N_{C1} and N_{C2} (count number per second [10]) at two threshold levels (giving total AE count and burst AE count).
The *in-situ* neutron diffraction tests were performed at high resolution two axis stress/strain diffractometer TKSN-400 at steady state reactor LVR-15.

Results and discussion

Strengthening effect of fibres

True stress-true strain curves obtained for the composite at various deformation temperatures are presented in Fig. 2. It can be seen that only at lower temperatures strain hardening is observed. At higher temperatures, the maximum stress = the ultimate compression strength (UCS) is observed at lower strains. Ductility

at low temperatures exhibits only several percent, at 200 and 300 °C about 10 or 20%, respectively. The values of the compressive yield stress (CYS) estimated for various temperatures are given in Table 1. For comparison, the values of the CYS estimated for the unreinforced alloy are also presented. The reinforcing effect of fibres estimated at room temperature exhibits 267 MPa and it decreases with increasing testing temperature up to 156 MPa at 300 °C.

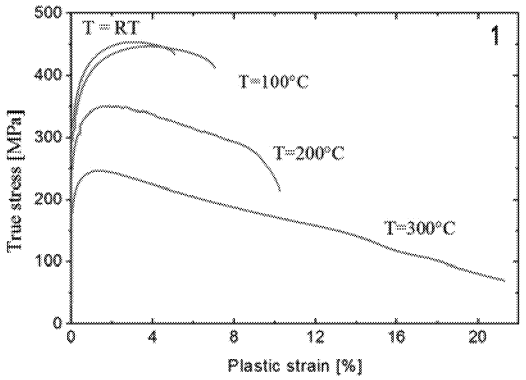

Fig. 2: Deformation curves measured at various temperatures.

	AJ51 alloy		AJ51+ Al_2O_3	
T (°C)	CYS (MPa)	UCS (MPa)	CYS (MPa)	UCS (MPa)
23	87	249	354	454
100	81	250	337	447
200	71	170	290	350
300	57	124	213	246

Table 1: The yield stress and ultimate compression strength estimated for the unreinforced alloy and composite.

Mechanism	
Load transfer	$\sigma_{LT} = \sigma_A\left[1+\frac{(L+t)\chi}{4L}\right]f+\sigma_A(1-f)$
Thermal mismatch	$\rho_T = \frac{Bf\Delta\alpha\Delta T}{b(1-f)}\frac{1}{t}$
Enhanced disl. density	$\Delta\sigma_D=\alpha_1\psi Gb(\rho_T+\rho_G)^{1/2}$
Geometrical dislocations	$\rho_G = \frac{f}{bt}8\varepsilon_p$
Orowan strengthening	$\Delta\sigma_{OR} = \frac{Gb}{\Lambda}+\frac{5}{2\pi}Gf\varepsilon_p$
Residual stresses	$\langle\sigma_m\rangle_{max} = \frac{2}{3}\sigma_y ln\left(\frac{1}{f}\right)\frac{f}{1-f}$
Hall-Petch strengthening	$\Delta\sigma_{GS} = K_y\left(d_2^{-1/2}-d_1^{-1/2}\right)$

Table 2: Individual contributions to strengthening following from the presence of the reinforcing phase.

σ_{LT}	ρ_T	ρ_G
L fibre length,t fibre thickness, σ_A alloy stress, χ=L/t	b Burgers vector, B=10 for fibres, $\Delta\alpha\Delta T$ thermal strain	ε_p plastic strain f volume fraction of fibres
σ_{OR}	$\langle\sigma\rangle$max	$\Delta\sigma_{GS}$
Λ distance between fibres	σ_y yield stress in the matrix	K_y Hall-Pech constant, d grain size

Table 3: Meaning of the quantities introduced in Table 2.

The difference between the stress necessary for deformation of the composite and the stress acting in the unreinforced alloy is a complex value containing various contributions due to the presence of fibres: (a) load transfer of the applied stress to the well bonded fibres [11] ($\Delta\sigma_{LT}$); (b) increase of the dislocation density accommodating the thermal stresses in the particle/matrix interface which are generated due to the difference of the coefficients of thermal expansion ($\Delta\alpha$) between matrix and particles [12] ($\Delta\sigma_{CTE}$); (c) increase in grain boundary area due to grain refinement – the Hall-Petch strengthening ($\Delta\sigma_{GS}$); (d) Orowan strengthening ($\Delta\sigma_{OR}$); (e) generation of geometrically necessary dislocations which accommodate the fibre/matrix interface during plastic deformation [13] ($\Delta\sigma_{GEO}$) and (f) residual thermal stresses $\Delta\sigma_{TH}$ (remaining in the matrix when stresses exceeding the yield stress are accommodated with newly created dislocations [8]. The stress σ_C necessary for the composite deformation may be expressed as

$$\sigma_C = \sigma_A + \Delta\sigma_{LT} + \Delta\sigma_{OR} + \Delta\sigma_{CTE} + \Delta\sigma_{GS} + \Delta\sigma_{GEO} + \Delta\sigma_{TH} . \quad (1)$$

Note that the plus sign has in this case only formal meaning, because indeed we do not know exactly, how to combine the individual strengthening terms [14]. The models briefly summarised in Table 2 (meanings of symbols used in Table 2 are given in Table 3) show that a composite strengthening depends on the geometrical parameters of reinforcements (size and shape of fibres or particles, volume fraction of the reinforcement, interparticle distance), on the physical properties of the components (thermal expansion coefficients, bonding at the interface matrix-reinforcement), on the microstructure and mechanical properties of the components. Contributions to the strengthening were calculated using model relationships introduced in Table 2. Results are summarised in Table 4. For calculation of the individual terms, the following constants were used: α(AJ51) = 26x10^{-6} K^{-1} (the own measurements), α(Saffil) = 6x10^{-6} K^{-1} [15], the shear modulus G = 17GPa, b = 3.2x10^{-10}m, K_y = 0.28 MPam$^{-3/2}$ [16], Taylor factor ψ [17], α_1=0.35 [18].

σ_{LT} (MPa)	ρ_T (m^{-2})	ρ_G (m^{-2})	$\Delta\sigma_D$ (MPa)	σ_{OR} (MPa)
63	2.8x10^{13}	3.0x10^{12}	64	3
$\langle\sigma\rangle_{max}$ (MPa)	$\Delta\sigma_{GS}$ MPa)	σ_m (MPa)	σ_{exp} (MPa)	σ_{theor} (MPa)
22	16	87	354	255

Table 4: Contributions of various strengthening mechanism to the yield stress of the composite at room temperature.

The effect of the load transfer is based on the existence of shear stresses at the interface between the matrix and the reinforcing phase fibres. It is calculated considering the perfect or nearly perfect bonding between the both components of the composite. The contribution to the load transfer can be calculated according to

$$\Delta\sigma_{LT} = \sigma_A \frac{(L+t)\chi}{4L} f \ , \qquad (2)$$

using the stress σ_A estimated for the unreinforced alloy. Because in this case all fibres are not aligned into the stress direction, they are randomly distributed in the fibres plane, only a component of this stress was applied $\Delta\sigma_{LT}.\beta$, where β is a mean value of the direction cosines.

From Table 4 it is obvious that the load transfer and enhanced dislocation density may significantly increase the composite flow stress. Other strengthening mechanisms are less important for the composite strength. Comparing the calculated value of the total stress with the experimental one it follows that the measured value is higher. The difference is approximately 100 MPa. This estimation is surprising because in the case of other magnesium alloys reinforced with short Saffil fibres the agreement was better and usually the calculated values of the composite CYS were higher than corresponding experimental values [19]. This fact may have these reasons:

i) It is not clear how to combine particular strengthening terms. In principle synergetic action may be considered.

ii) Models for composite strengthening consider the uniform distribution of the reinforcing phase fibres (or particles). As it can be seen in Fig. 1 this condition is not fulfilled.

iii) Contributions to strengthening were not exactly calculated. Probably the equations used are too simple and it is necessary to take into account more aspects. Thermal stresses induced into matrix and load transfer depend strongly on the quality of the interface bonding [20]. It is possible that the residual thermal stresses and load transfer are higher that the calculated values.

To check the possibility that the residual thermal stresses are higher, neutron diffraction (ND) measurements were performed. Strain/stress measurement by neutron diffraction is a non-destructive technique that uses the diffraction of a beam of thermal neutrons to determine the atomic spacing within a small gauge volume inside polycrystalline materials.

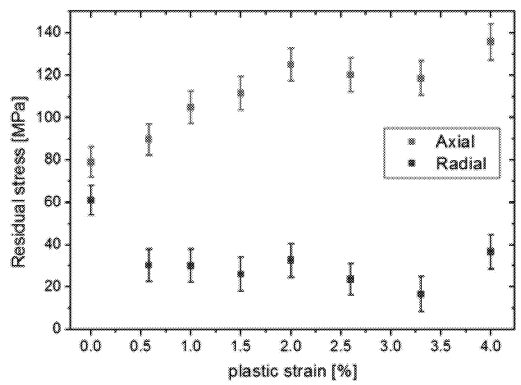

Fig. 3: Residual stresses estimated in axial and radial directions.

The strain dependence of residual stresses estimated using ND in both axial and radial directions in the cylindrical sample are shown in Fig. 3. Performing correction using value of the residual thermal stress estimated using ND the resulting theoretical stress necessary for deformation of the composite at room temperature is 311 MPa that is closer to an experimental value of 354 MPa.

Deformation mechanisms

It is generally accepted that during straining of a composite, deformation occurs in the matrix and short ceramic fibres deform only elastically. Deformation of the *hcp* AJ51 matrix alloy may be realised by the dislocation motion in basal and non-basal planes as well as by mechanical twinning. The hardening processes are connected with the storage of dislocations on non-dislocation and dislocation type obstacles. In the case of composites, different obstacles for the dislocation motion in the matrix should be considered. There are a) non-dislocation obstacles such as grain boundaries, precipitates, short fibres and b) dislocations in different slip systems – the dislocation forest. On the other hand, the moving dislocations can cross slip and/or locally climb; these are mechanisms leading to a decrease in the dislocation density. Introducing the reinforcing phases into the metal matrix influences not only the densities of the thermally formed and geometrically necessary dislocations, but also the dislocations stored at reinforcements during deformation. Considering these effects, the total dislocation density in composites can be written:

$$\rho_{total} = \rho_T + \rho_G + (\rho_S + \rho_a), \qquad (3)$$

where ρ_S is the statistically stored dislocation density in unreinforced matrix, ρ_a is the diminished part of the statistically stored dislocations due to the addition of a reinforcing phase. The strengthening in the matrix is attributed to the deformation resistance induced by the reinforcing phase. According to the Taylor relation, the contribution to the total stress due to the presence of dislocations in the matrix may be written:

$$\Delta\sigma_D = \alpha_1 \psi G b \left(\rho_T + \rho_G + \rho_S + \rho_a\right)^{1/2} . \qquad (4)$$

This higher matrix dislocation density as well as the reinforcement/matrix interfaces can provide high diffusivity paths in a composite. Such possibility may play an important role in the softening process(es).

To reveal details of the deformation mechanisms operating during straining of AJ51 alloy reinforced with short Saffil fibres AE measurements have been used. The true stresses plotted against the true strain together with the strain variation of the AE count rates and amplitudes of the AE signals are shown in Fig 4 for the matrix alloy (a) and composite (b). The strain dependence of the AE signal has its characteristic course usually observed in metallic polycrystals with the pronounced maximum at the beginning of the straining followed with the rapid decrease of the AE. Observed peak of the AE signal at the low strain can be described to the twin formation and collective motion of dislocations [21]. On the other hand, during deformation of composite, two different maxima of the AE activity are observed. A higher activity of the AE at the beginning of the straining decreases with increasing strain. The second lower local maximum is observed at a higher step of straining before the composite failure.

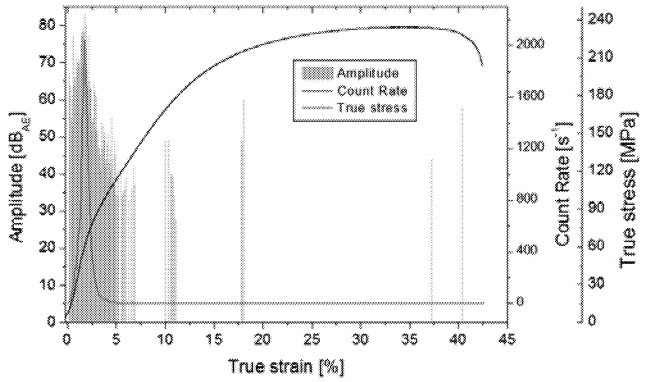

a)

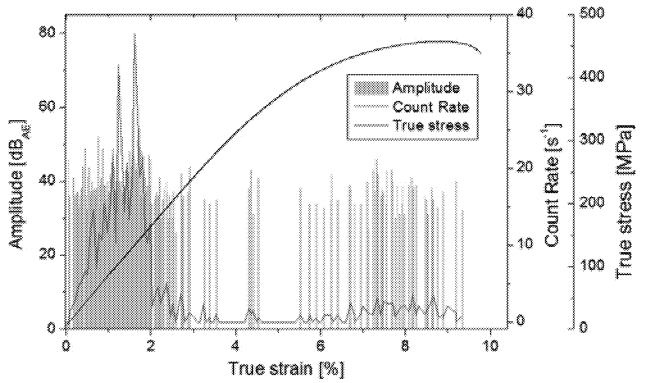

b)

Fig. 4: Count rates and amplitudes of the AE signal recorded during plastic deformation of the matrix alloy (a) and composite (b) at room temperature and strain rate of $10^{-3}s^{-1}$.

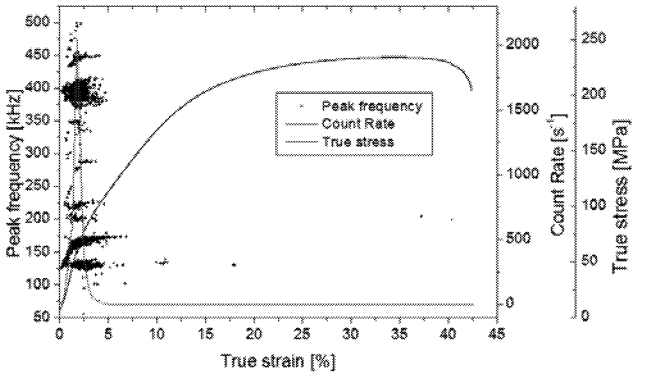

a)

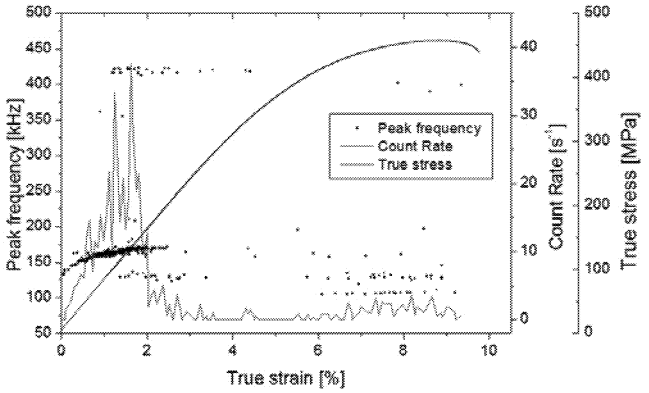

b)

Fig. 5: Characteristic frequencies of the AE signal estimated for the matrix alloy (a) and composite (b).

The first peak of the double maximum at the deformation beginning is connected with of the generation of the primary twins $\{10\bar{1}2\}\langle 10\bar{1}0\rangle$ [22]. According to Klimanek and Pötsch [23] the second peak may be attributed to the secondary twins' production in the $\{10\bar{1}1\}\langle 10\bar{1}2\rangle$ system. Following decrease of the AE activity in the alloy and composite is connected with the growth of twins. Such mechanism has substantially lower AE response comparing with the twins nucleation. The observed increase in the AE activity in the composite close to the end of the stress-strain curve is connected with the breakage of fibres. The fibres may be also pulled out from the matrix, which is also a possible source of the AE signal. Note that results obtained for the alloy and composite are not directly comparable. Both materials have different grain size; the mechanical twinning is strongly dependent on the grain size [24], the comparison of the alloy with composite can be made only qualitatively. Characteristic frequencies of the AE signals were estimated using Fast Fourier Transform. 180 kHz and the higher frequency range from 370 up to 450 kHz (see Fig. 5). Results are shown in Fig. 5a for the alloy and 5b for the composite.

Two main frequency intervals were observed; 130-180 kHz and a higher frequency range from 370 up to 450 kHz (see Fig. 5).
Li and Enoki [25] considered that the signals characterised with the higher frequencies originate from the twins nucleation while the lower frequencies are characteristic for glide of dislocations. Characteristic frequencies estimated during plastic deformation showed that the early stages of the plastic deformation of the alloy are realised with both slip of dislocation ensembles and mechanical twinning. In the composite the role of twinning is not so important Increasing dislocation density and relatively low grain size (with respect to twinning) in the composite could indicate that the dislocation motion is more significant during deformation of the composite.
Experiments with the AE measurements were repeated at an initial strain rate of 10^{-4} s^{-1}. The results are shown in Fig. 6a for the matrix alloy and 6b for the composite. Differences between both results presented in Figs. 5 and 6 for both materials may be easily estimated. It is clear that in this case the twinning plays more important role in both materials in comparison with results obtained at the higher strain rate. The obtained results indicate a significant sensitivity of the twins´ formation to the strain rate.

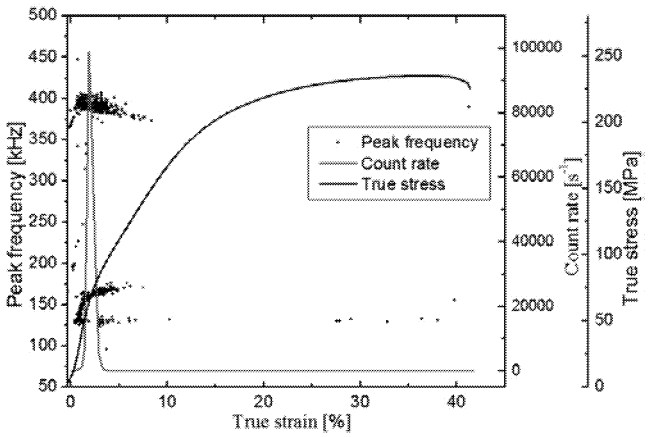

a)

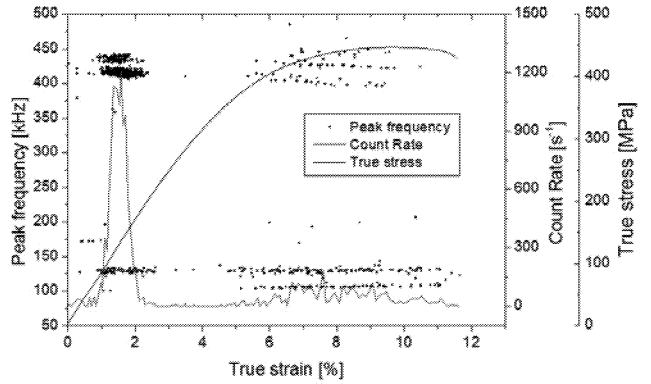

b)

Fig. 6: Characteristic frequencies of the AE signal estimated for the matrix alloy (a) and composite (b). The strain rate used was $10^{-4}s^{-1}$.

Conclusions

Magnesium alloy AJ51 and AJ51 alloy reinforced with 17.9 vol. % of short Saffil fibres were deformed at various temperatures from room temperature up to 300 °C. Samples for deformation were cut from the castings so that the fibre plane was parallel to the stress axis. During deformation at room temperature, the acoustic emission signal was measured at two strain rates. Strengthening effect of fibres was analysed. An increase in the dislocation density and load transfer were found as the significant contributions to the fibres strengthening. Neutron diffraction revealed high level of the residual stresses in the composite matrix. In both alloy and composite pronounced maxima of the AE signal at the onset of plastic deformation; in the composite additional maximum of the AE activity was observed in the vicinity of the maximum stress. This maximum was described to the fibre breakage and pulling out of fibres. Fast Fourier Transform of the AE signal showed that the AE signal frequency exhibits two regions. Lower frequencies may be described to the glide of dislocations while the twins´ nucleation can be characterised with higher frequencies. The activity of both mechanisms is sensitive to the strain rate.

Acknowledgements

The authors are grateful for the financial support of the Czech Grant Agency under the contract P108/12/J018.

References

[1] T.W. Clyne and P.J. Withers: *An Introduction to Metal Matrix Composites*, (Cambridge, Cambridge Univ. Press, 1993).

[2] N. Chawla and K.K. Chawla: *Metal Matrix Composites.* (New York, Springer Verlag, 2006).

[3] M.J. Koczak, S.C. Khatri, J.E. Allison and M.G. Bader: Fundamentals of Metal Matrix Composites (Eds. S. Suresh, A. Mortensen, A. Needleman), Butterworth-Heinemann, Boston, MA, 1993. 297-326.

[4] S. Roy et al., "Complete Determinativ of Elastic Moduli of Interpenetrating Metal/Ceramic Composites Using Ultrasonic Techniques and Micromechanical Modelling" *Materials Science and Engineering A*, 528 (2011), 8226–8235.

[5] Z. Trojanová et al., "Mechanical and Fracture Properties of an AZ91 Magnesium Alloy Reinforced by Si and SiC Particles", *Composites Science and Technology,* 69, (2009), 2256–2264.

[6] Z. Trojanová; et al., "Strengthening in Mg–Li Matrix Composites", *Composites Science and Technology*, 67 (2007), 1965–1973.

[7] Y. Ochi et al., "Effects of Volume Fraction of Alumina Short Fibers on High Cycle Fatigue Properties of Al and Mg Alloy Composites", *Materials Science and Engineering A*, 468-470 (2007), 230–236.

[8] F. Delannay: Comprehensive Composite Materials, Vol. 3, (Elsevier, Amsterdam; Ed. T.W. Clyne, 2000) 341–369.

[9] M. Kunst et al.: Creep Deformation and Mechanisms of AJ (Mg-Al-Sr) alloys. *Proc. of Inter. Symposium on Magnesium Technology in the Global Age.* Canad. Inst. of Mining, Metallurgy and Petroleum, Montréal, Canada (2006) 647–661.

[10] Standard Practice for Acoustic Emission Examination of Fiberglass Reinforced Plastic Resin, (ASTM E. Tank/Vessels: May 31, 1985), 1067–85.

[11] R.M. Aikin, Jr. and L. Christodoulou, "The Role of Equiaxed Particles on the Yield Stress of Composites", *Scripta Metallurgica et Materialia*, 25 (1991), 9-14

[12] R.J. Arsenault and N. Shi, "Dislocation Generation due to Differences between the Coefficients of Thermal Expansion", *Materials Scence and Engineerig.*, 81, (1986), 175-187.

[13] M.F. Ashby, "Criteria for Selecting the Components of Composites". *Acta Metallurgica et Mateialia*, *41*, (1993), 1313-325.

[14] H. Lilholt, "Aspects of Deformation of Metal Matrix Composites", *Materials Science and Engineering A*, 135 (1991), 161-171.

[15] D.R. Like and B. Raton Eds. Handbook of Chemistry and Physics. 73rd edition. (CRC Press, USA, 1992-1993)

[16] M. Mabuchi and K. Higashi, "Strengthening in Mg-Si Alloy", *Acta Materialia*, 44, (1996), 4611-4618.

[17] R.W. Armstrong, " Theory of the Tensile Ductile-Brittle Behaviour of Polycrystalline hcp Materials with Application to Beryllium", *Acta Metallurgica*, 16 (1968), 347-355.

[18] F.F. Lavrentev, Y.A. Pokhil and I.N. Zolotukhina, "Analysis of Pairwise Dislocation Interaction and its Contribution to Flow Stress during Magnesium Crystal Basal Slip", *Materials Science and Engineering*, 32 (1978), 113-119.

[19] Z. Trojanová et al., ”Magnesium Alloys Based Composites”, *Magnesium alloys-Design, Processing and Properties*. (Ed. F. Czerwinski, INTECH 2011) 501-526.
[20] Z. Trojanová et al., ”Influence of Thermal and Mechanical Cycles on the Damping Behaviour of Mg Based Nanocomposite”, *Fatigue behaviour of fiber reinforced composites. Experiments and simulations.* (W. Yao, J. Renard, N. Himmel Eds., Lancaster, USA, Destech Publications, Inc. 2012,) 239–248.
[21] M. Janeček et al., ”Mechanisms of Plastic Deformation in AZ31 Magnesium Alloy Investigated by Acoustic Emission and Transmission Electron Microscopy”, *Materials Science and Engineering A,* 462 (2007), 311–315.
[22] Z. Trojanová, Z. Száraz, F.Chmelík, P. Lukáč ” Acoustic Emission from Deformed Magnesium Alloy based Composites”, *Materials Science and Engineering A,* 528 (2011), 2479–2483.
[23] Klimanek P, Pötzsch A. ”Microstructure Evolution Under Compressive Plastic Deformation of Magnesium at Different Temperatures and Strain Rates”. *Materials Science and Engineering A* 324 (2002), 145–50.
[24] Máthis et al., ”Investigation of Tension–Compression Asymmetry of Magnesium by Use of the Acoustic Emission Technique”, *Materials Science and Engineering A* 528 (2011), 5904–5907.
[25] Y. Li and M. Enoki, ”Twinning Behavior of Pure Magnesium Quantitatively Investigated by Acoustic Emission*”, Materials Science and Engineering A,* 536 (2012), 8–13.